Design of a composite carbon fibre wheel for a motorcycle

Gonçalo A. L. Pereira

Mechanical Engineering Department

Instituto Superior Técnico (IST)

goncalopereira_dh11@hotmail.com

ABSTRACT

Design of a composite wheel for a motorcycle composed by different essential parts taking in consideration the manufacturing method and function. The manufacturing method was developed in line with the design of the part. Standards were used to get the rim contour and alloy wheel load requirements in order to assure that the wheel fulfils certification entities requests. The materials used in the assembly of parts were a carbon fibre reinforced plastic to the wheel and an aluminium alloy to the hubs. A topology optimization was made to the hub in order to obtain a stiffness optimized structure to the manufacturing constraints and an optimization methodology for carbon fibre reinforced plastic was developed to this kind of geometry in order to obtain ply shapes, thickness and stacking sequence. To improve the results of the finite element method, quadratic elements were used in the final optimized model of the wheel for better approximation of the results.

Keywords: Motorcycle, Wheel, Optimization, Composites, Carbon fibre

I. INTRODUCTION

The aim of this work is the idealization and design of a front motorcycle wheel and every component needed for its correct function in a road/racing application. The manufacturing method was created during the design, having in mind construction details and the utilization from the rider. Optimization methods were used in order to achieve a rigid and light design. A search of what's available in the market today was made in order to get reference values, such as mass and inertia moment of rotation, getting the values: 2,5 kg and 63500 kg.mm^2 respectively. The wheel must be made in accordance to what is used in the target motorcycles, such as having two brake discs, fit common tire size, have common wheel diameter, easy manufacturing and it needs to be adaptable to every motorcycle manufacturer. The tire used is tubeless with reference dimensions "*120/70 R 17".*

A. Geometry requirements

To start, some basic geometry must be defined such as spoke number, rim contour and the hub. The spoke number was defined as the number of bolts from the disc brake. This way a linear and similar load path is possible, as the hub will have a cyclic symmetrical load distribution from braking torque. The rim contour was made in accordance to the ISO standard [1]. A well contour option presented was used in order to facilitate tire assembly. To fit every motorcycle manufacturer, a hub change is possible as the wheel is separable from the hub, a different hub measure will provide the different fit dimensions.

B. Mass and moment of inertia

As a wheel rotates along with the direction of travel, the presence of the steering generates a gyroscopic effect. This effect has influence in different parameters, but in accordance to section 4.14 found in [2], the contribution to lean the motorcycle to a turn is minor and the stability is majorly achieved with suspension geometry such as rake angle and trail. This way the wheel inertia moments major influence is in the steering torque input, which diminishes with inertia, but the output increases with the perturbations of the road. The ability to accelerate and brake the motorcycle, is also a little better in accordance with the equations (1) and (2), which describes the kinetic energy (E_c) present in a wheel while moving and the torque (M) needed to accelerate or brake the wheel, respectively.

$$E_c^W = 0{,}5 * m_W * v_W^2 + 0{,}5 * I_W * w_W^2 \ [J] \quad (1)$$

$$M_Z = I_W * \alpha_W \ [N.m] \quad (2)$$

where *m* represents the mass, *I* the rotational inertia, *v* the linear velocity, *w* the angular velocity and *α* the angular acceleration of the wheel.

C. Compliance and wheel vertical rigidity

In order to maximize traction and road-holding parameters of the motorcycle, rigid components must be used. An analysis must be made on how rigid the part has to be in accordance to its importance to these parameters. Compliance of components affects the system natural frequencies, absorbs the dynamic loads that should go to the suspension and tire, change motorcycle geometry parameters and inhibit proper tire support. Having in mind that the stiffness must be high enough to neglect the contribution of the wheel in the system, a simple approach can be made considering a series of springs composed by the tire (K_t) and wheel (K_w). The equivalent stiffness (K_{eq}) of this two springs is showed in equation (3).

$$K_{eq} = \frac{K_w * K_t}{K_w + K_t} \qquad (3)$$

Normalizing the equation (3) to the tire stiffness and plotting it, we get Fig. 1, which shows that with a $K_w/K_t > 20$ the influence of the wheel stiffness is around 5%, which can be neglected. As a reference, this must be checked in the optimization for a tire with a high stiffness value, obtaining the wheel stiffness by dividing the vertical load applied by the maximum displacement in the rim contour.

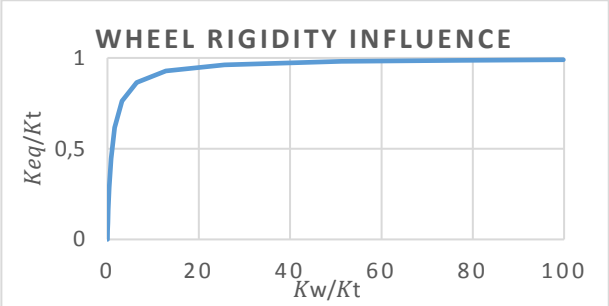

Fig. 1 - Wheel vertical rigidity influence

D. Optimization

In order to proceed to the optimization, the constraints must be defined. To achieve a rigid structure and facilitate the optimization procedure, it was decided to minimize compliance (*C*) as a first step. This is equal to the elastic strain energy, *U,* as showed in equation (4) taken from [3]. In a presence of more than one load case, the compliance sumation is used.

$$C = 0{,}5 * \boldsymbol{u}^T * \boldsymbol{f} = U\ [N.m] \qquad (4)$$

where *u* represents the displacement vector and *f* the load vector.

If minimizing compliance is used, it's possible to achieve a structure when the exact load cases are not defined. As this is a component that has its loads changing direction and magnitude at every moment, because it's rotating, a mass minimization would reduce material where it may be needed. Even implementing constraints that force the keep of material, a reduction that would not be beneficial will occur in some areas. As the stresses are filtered in a topology or free-size optimization, displacement or strain energy could produce a safer structure with sufficient material everywhere, but there were no reference values so this option was abandoned. The optimization process of the wheel was divided in 5 steps: the hub topology, wheel spokes inclination, wheel ply shapes, thickness and stacking sequence. The solver used in the optimization was "*Optistruct*", described in [3]. An optimization problem is defined with an objective function:

$$\min_x f(x) = f(x_1, x_2, x_3, \dots) \qquad (5)$$

Subject to:

$$g_j(x) \leq 0, \qquad j = 1, \dots, m \qquad (6)$$

$$x_i^L < x_i < x_i^U, \qquad i = 1, \dots, n \qquad (7)$$

Where $g_j(x)$ represents the *j* constraint and x_i the *i* design variables.

II. METHOD AND RESULTS

A. Load cases

The load cases were obtained using the ISO standard presented in [4]. This is an alloy-wheel standard, but it was used because a composite wheel standard was not found. The brake torque used was 50% higher as the one presented in the standard. This was decided by racing data obtained in [5]. The load application points in the wheel are presented in Fig. 2, one centred with one spoke and the other between two spokes.

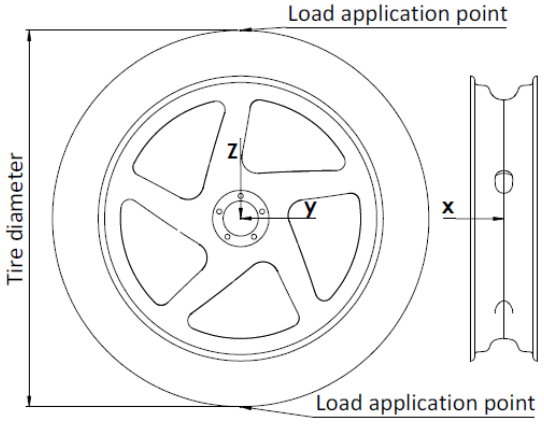

Fig. 2 - Load application points

Table 1 - Wheel load cases used

Vertical		Lateral			Braking		
Z [N]	Pressure [MPa]	Z [N]	X [N]	Pressure [MPa]	Z [N]	Y [N]	Pressure [MPa]
5518	0,41	1203	1203	0,41	2158	3885	0,41

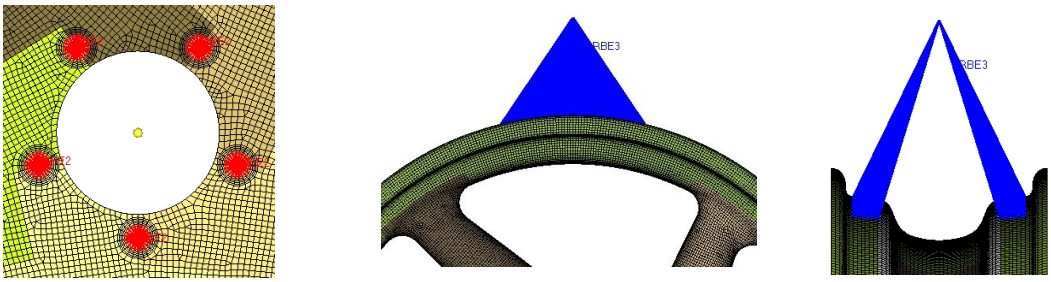

Fig. 3 - Wheel constraints and loads

The final load cases are presented in Table 1, considering also the maximum tire pressure in the entire rim contour. With three load cases and two load application points, six load cases were used. From this load cases applied in the points showed in Fig. 2, the forces were transposed to the hub. The constraints used are presented in Fig. 3, fixed in all directions in the hub bolt holes. The loads were applied via *"RBE3",* a kind of rigid element which does not induce rigidity to the part. As this is a part which will be used until failure without control, a high safety factor must be used. Reliable fatigue data were not available to the author, so as reference, a notched quasi-isotropic carbon fibre composite, has a $\sigma_{Max}/\sigma_{Ult} = 0{,}6$ threshold taken from [6]. This ratio means the maximum fatigue strength dividing by the ultimate strength of the composite. Considering the type of unpredictable use of the part, a static safety factor of 3 was used.

B. Hub topology

Some attempts were made to get the initial design volume, in order to achieve an easy and quick manufacturable design by a CNC process. The objective function used was the sum of the compliance of all load cases with mass, moment of inertia and cyclic symmetry as constraints. These values were obtained with iterations of the model parameters. The process is showed in Fig. 4.

C. Wheel spokes inclination

With this optimization, the goal is to get an inclination angle which produces axial traction loads reducing deflection in the spokes, as these are the most suitable for fibres. This is possible because the front wheel only has braking torque and not acceleration torque, otherwise a compromise between the two needed to be made. A simple model with 1D-beam elements as spokes with a tube cross section was made, simulating the wheel. Two circles simulated the position of the element nodes, as rim contour and a rigid hub. This last modelled with rigid elements to apply the loads. The outer one is fixed and the inner one is able to rotate as a design variable. In order to get an inclination angle, different area and inertia cross sections, brake torque magnitude, vertical force in the hub in two different directions and hub diameter were used to get a relation with the optimized angle. This proved to have little effect and the median value was used. The objective function used was the compliance to achieve a rigid structure, diminishing spoke moments, with the goal to achieve traction load in the spokes. The process of optimization used is briefly showed in Fig. 5. The first image represents the model, the second the limit of rotation of the inner hub and the third is the final inclination.

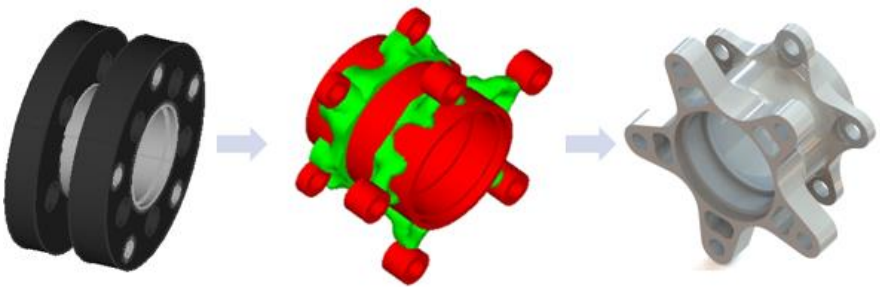

Fig. 4 - Hub topology model and result

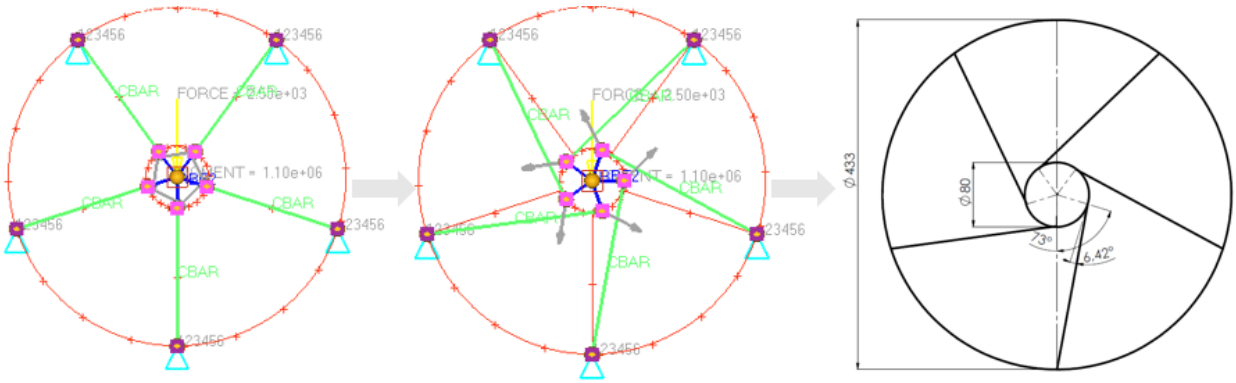

Fig. 5 - Spoke inclination angle model and result

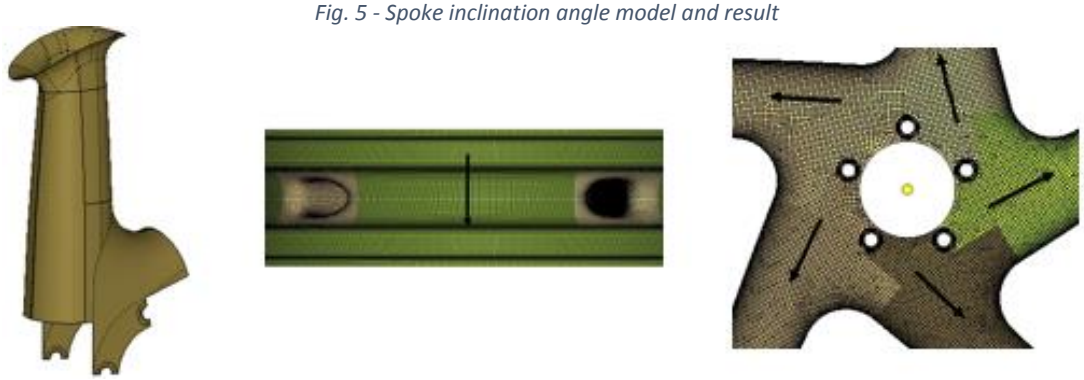

Fig. 6 - Spoke division and fibre orientation

D. Ply shapes

A free-size optimization was used to get the ply shapes. As this is a cyclic geometry, different coordinate system must be used in every spoke to get cyclic symmetry between spokes. In order to use global plies to facilitate this early process, the geometry must be divided equally into sections. These sections will be the rim contour and five spokes, including the hub. This way, the zero-degree plies are aligned with the axle of each spoke to simplify the manufacturing process. The division into sections is important as it will be used in the staking sequence optimization as well. This division is showed in the first image of Fig. 6. The other two images refer to the zero-degree element coordinate system used in the rim contour and spokes. As an initial laminate, four plies were used with a thickness of 2 mm each, with the stacking sequence [0°, ±45°, 90°] with the orientation aligned with element coordinate system. These plies cover the entire surface of the wheel. To simplify this first stage optimization, the stacking sequence can be ignored by using the smeared stiffness-based method, presented in [7]. This is an approach that aims to neutralize these effects by considering homogenous sections with quasi-isotropic layups. This method is used to calculate the laminate constitutive matrices ***A***, ***B*** and ***D*** without determining a stacking sequence. These simplified equations are presented in equations (8), (9) and (10).

$$\boldsymbol{A}_{\boldsymbol{ij}}^{*} = \sum_{k=1}^{n} \overline{\boldsymbol{Q}}_{ij}^{k} \left(z_k - z_{k-1}\right) \tag{8}$$

$$\boldsymbol{B}_{\boldsymbol{ij}}^{*} = 0 \tag{9}$$

$$\boldsymbol{D}_{\boldsymbol{ij}}^{*} = \boldsymbol{A}_{\boldsymbol{ij}}^{*} * \frac{t_{Lam}^{2}}{12} \tag{10}$$

where $\overline{\boldsymbol{Q}}$ is the layer stiffness matrix in global coordinate system, z_k the thickness coordinate of the ply and t_{Lam} the laminate thickness.

The areas represented in colours different than grey in Fig. 7, were constrained to have constant thickness. This enables to have proper tire contact to avoid lost tire pressure and hub constant thickness needed to the manufacturing process.

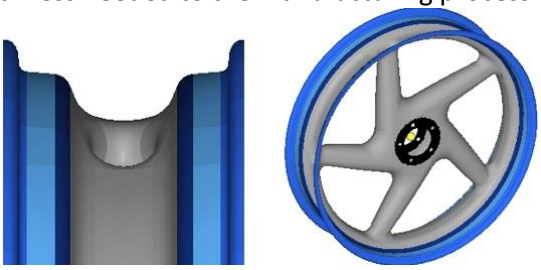

Fig. 7 - Constant thickness areas in the wheel

The objective function used was the sum of the compliance of all load cases with mass, moment of inertia, cyclic symmetry, minimal thickness of 1 mm and a balanced laminate in the ±45° plies as constraints. These values were obtained with iterations performed to the model parameters and some reference values.

The result obtained from this optimization is showed in Fig. 8, being the details 1 and 2 ignored. Detail 1 were introduced by the RBE3 element forces and detail 2 due the constant thickness distribution in the hub area. To get the ply shapes, an analysis of the thickness distribution by orientation result was made. This way it was easier to get ply shapes where high thickness is needed. This is showed in Fig. 9.

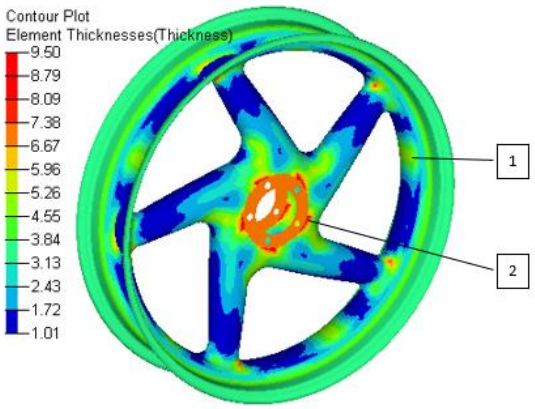

Fig. 8 - Thickness distribution obtained in free-size optimization

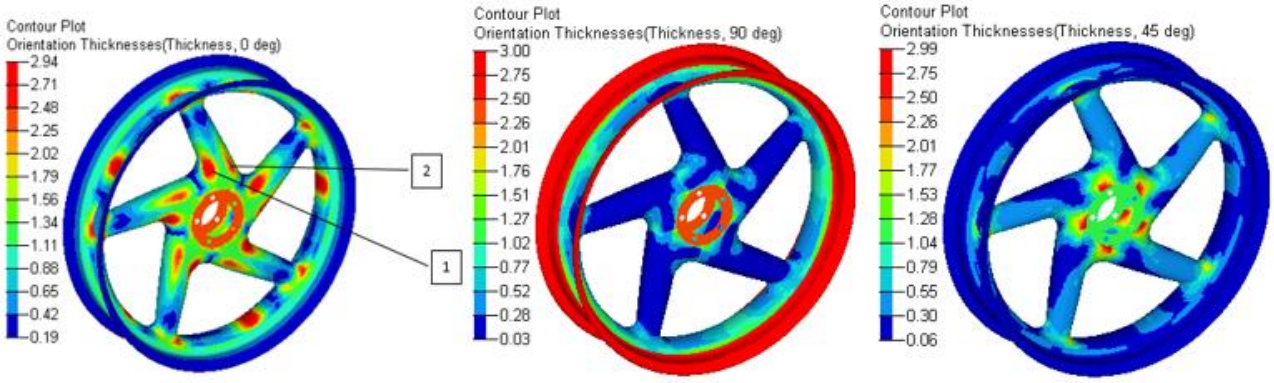

Fig. 9 - Thickness distribution by orientation

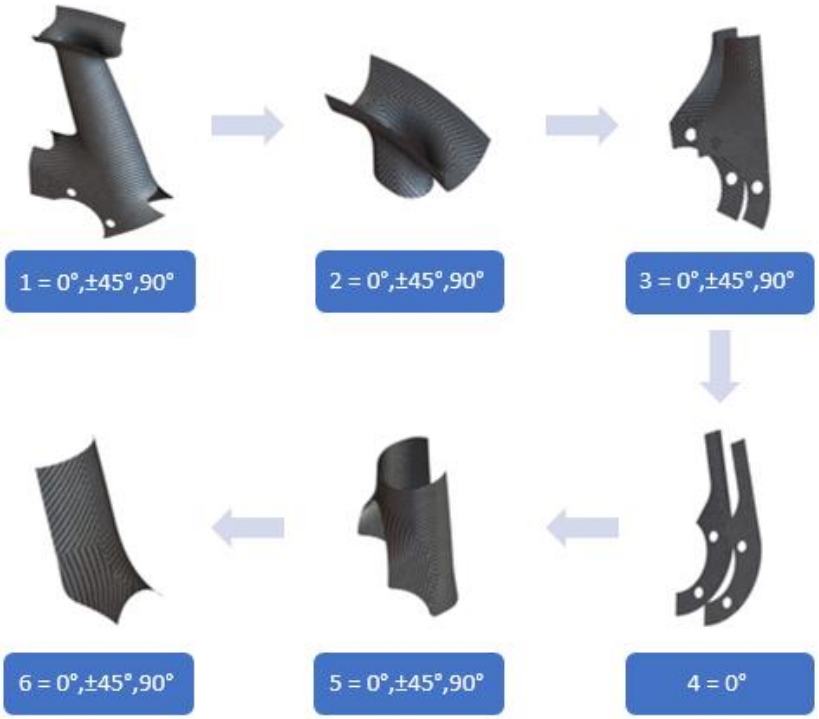

Fig. 10 - Ply shapes in the spokes

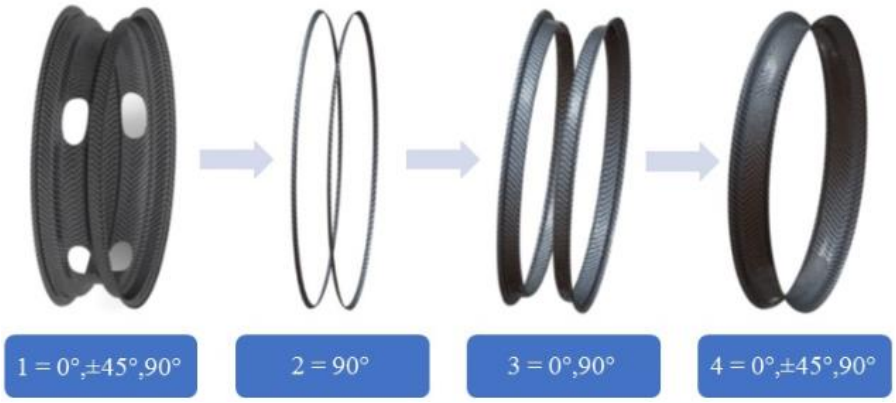

Fig. 11 - Ply shapes in the rim contour

With these results, the ply shapes were determined by hand, thinking in manufacturing and reinforcement needed. These ply shapes are presented in Fig. 11 for spokes and in Fig. 10 for the rim contour. Some of these shapes will be divided into multiple plies to enable manufacturing, as the 1 and 2 reinforcements presented in Fig. 10 and all the plies in the rim contour presented in Fig. 11 are not manufacturable. These divisions were not implemented in the model as this won't have any effect in the FEM formulation. Both Fig. 10 and Fig. 11, present the reinforcement identification number and the orientation used for each shape.

E. Ply thickness

In order to get ply thickness, a model was made considering the ply shapes obtained. Every spoke has one ply of each shape and orientation, with an initial thickness of 2 mm. The same was made in the rim contour. Using a design variable for each ply shape orientation enables to get cyclic symmetric result, and using the same design variable for ±45° plies enables balance of orientation as a design requirement. Being the design variables the thickness of plies, they can only take a multiple value of the carbon fiber fabric thickness. This enables to calculate the number of plies that will be used in every reinforcement. Instead of an element coordinate system, a ply coordinate system was used aligned as presented in Fig. 6. This enables the consideration of the overlapping ply area correct orientation. In this optimization, it is possible to accurately calculate a failure index of the material, so it was used as a constraint and this enables to use mass as an objective function. This way the design will be optimized to save weight. A moment of inertia, minimum thickness of 8 plies in every element and a sum of compliance obtained earlier was used as constraints.

The fiber failure index used was *Tsai-Hill,* because it enables to calculate a safety factor easily, and a simple linear inter-laminar criterion based in the first order shear deformation theory of laminated plates explained in [8] was used. The model was implemented considering the stacking sequence with the Classical laminate theory material equations, taken from [8]. This enables to get correct results for the failure indexes. The result obtained in thickness distribution is presented in Fig. 12 and the number of plies that need to be used of each reinforcement and orientation are presented in Fig. 13, having a total number of 182 plies.

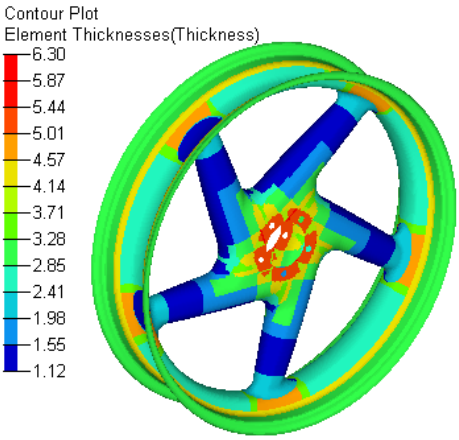

Fig. 12 - Thickness optimization of the plies

Spokes		Orientation		
		0°	45°	90°
Reinforcement	1	3	2	2
	2	3	1	1
	3	5	1	1
	4	1	0	0
	5	1	1	1
	6	1	0	1

Rim contour		Orientation		
		0°	45°	90°
Reinforcement	1	2	1	6
	2	0	0	3
	3	0	0	11
	4	5	1	1

Fig. 13 - Ply quantity of each reinforcement and orientation

F. Ply stacking sequence

To enable a meaningful analysis, the plies of the same reinforcement and orientation in the spokes must be laid up together in the geometry and ply crossing must be avoided.

To model these problems, the grouping of similar spoke plies into one and six stacking design variables were implemented. To enable the grouping of plies the element coordinate system used is the same as in free-size optimization for simplification. As an example, the spoke reinforcement number 3 is presented as one ply in Fig. 14 as used in this model. This grouping reduced the number of plies from 182 to 67 reducing computational effort and enabling this analysis.

Fig. 14 - Ply reinforcement 3 present in the spokes

Plies were grouped together as sets, as demonstrated below:

1) Reinforcement of the rim contour: number 1,2 and 3: (Total of 24 plies), Order [1-24];
2) Reinforcement of the spokes: number 1 (±45° plies); (Total of 2 plies), Order [25-26];
3) Reinforcement of the spokes: number 1, 3, 4; (Total of 15 plies), Order [27-41];
4) Reinforcement of the spokes: number 2; (Total of 6 plies), Order [42-47];
5) Reinforcement of the spokes: number 1 (one 90° ply), 5, 6; (Total of 7 plies), Order [50-56];
6) Reinforcement of the rim contour: number 4; (Total of 8 plies), Order [60-67];

Ply_x_1.x_2.x_3.x_4	x_1 = Zone	Spokes = 1, Rim contour = 2
	x_2 = nº of Reinforcement	1 - 6, 1-4
	x_3 = Ply orientation	1 = 0°, 2 = 45°, 3 = -45°, 4 =90°
	x_4 = nº of Ply	1,2,3,...,11

Fig. 15 -Ply identification system

The division into six sets of plies were made to reproduce the stacking sequence needed for the manufacturing method. These sets simplify the model, enabling the achievement of a converged result and ply crossing free design, otherwise not possible. A design variable was introduced to each ply set. This way, a stacking sequence optimization is performed to each set. The objective function used was the sum of the compliance of all load cases, as mass won't change because the only thing changing is stacking sequence. As constraints, the maximum number of consecutive plies was set to 4, grouping of ±45° plies and a failure index of 0,28 must be achieved. This failure index was obtained by iterations as the geometry does violate the failure index target for this part in some elements. To diminish this, some elements were taken out from the analysing list and the failure index target was raised to achieve a converged result. A ply identification system must be used to identify the stacking sequence. This is presented in Fig. 15. The final stacking sequence is presented in Fig. 16. The different colours indicate the ply orientation for easy reading. The laminate lay-up starts from set 1 to set 6 in relation to the mold surface.

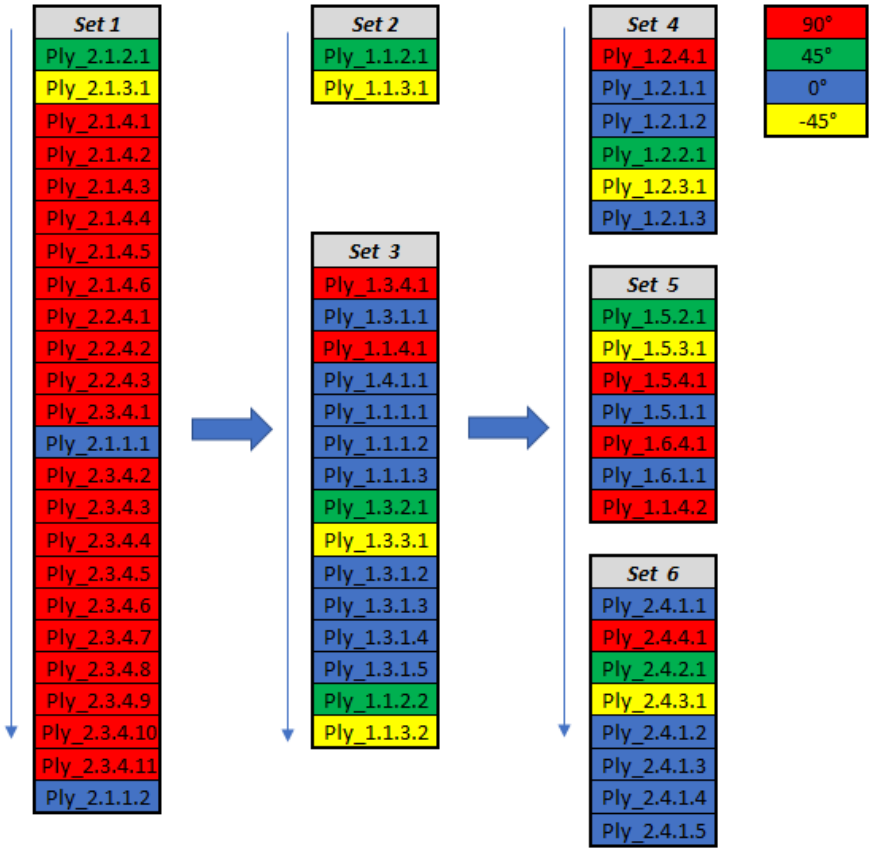

Fig. 16 - Final stacking sequence of plies

G. Stress analysis

In the hub, tetrahedral elements were used for simplicity. This enabled the use of a simpler and faster software to get results. Refining the mesh where needed, it compensates the fact that these elements have constant strain field. This is not desirable. However, the factor of safety is very high and it was assumed safe from previous experiences.

In the composite material, a reliable result is needed. A mesh convergence study was the first thing performed, this with an isotropic material. As the model progressed, it was very labour intensive to redo the mesh as the elements in the plies needed to be selected all over again. To simplify this, an element order formulation change was made, changing from linear to quadratic. This enabled to get a more converged and precise result.

- *Wheel*

Both Fig. 17 and Fig. 18 show composite failure index of two different load cases, which is the maximum of the fiber and inter-laminar criteria.

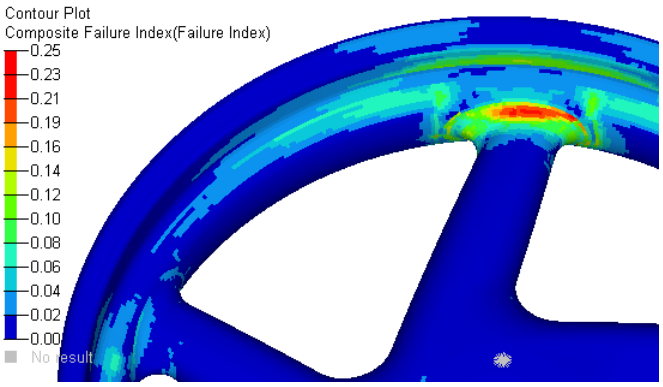

Fig. 17 - Vertical load case centred with spoke

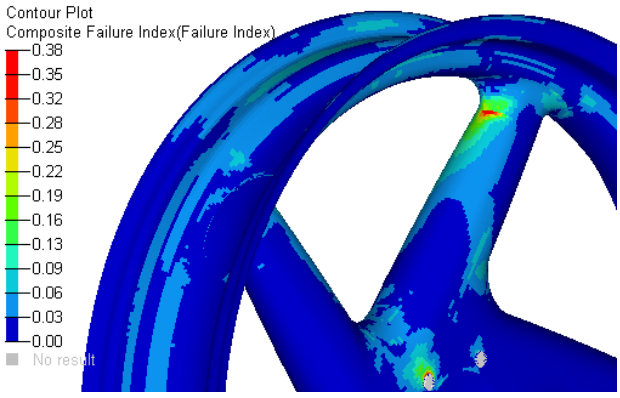

Fig. 18 - Lateral load cases between spokes

Due to some simplifications on the load application, some regions have high failure indexes, however this is safely below the limits. This happens because the load is distributed in a much smaller area than the real case. The highest failure index is present in the lateral load case between two spokes.

In Fig. 17 the highest value is present in a three-surface intersection line. There are a few elements attached to this border. Being this a singularity, this result was accepted. Besides the fillet with a low safety factor (around 2) showed in red colour, all the green areas are within the desired safety factor.

In Fig. 18 the highest value is present in the ply drop of the reinforcement fillet plies. This being also a singularity, the value was accepted. The elements with green colour have a safety factor of around 2,3.

All these high values are in the fibers, being the inter-laminar stresses low compared to the fiber values.

- *Hub*

To stay below the fatigue stress limit of the material, the stress must not pass 133 MPa from the material data used. The result has a factor of safety to yield superior to 3, and above 1 to fatigue considering R = -1. As it can be seen from Fig. 19, the elements with stresses above 100 MPa are very localized areas with some higher values due to constraints or sharp edges.

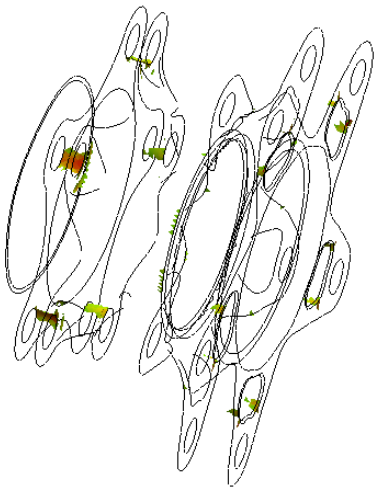

Fig. 19 - Hub stresses superior to 100 MPa

III. DISCUSION OF RESULTS

The stress analysis of the wheel shows some low values for the safety factor. The method of applying the load is not ideal as it does not spread the load over the real area. This concentrates a lot of load in one spoke when the load is aligned with it and in the fillets when applied between spokes.

Also, the lateral load case, which is the worst, is difficult to occur as the motorcycle leans to the corners.

The safety factor is also very high, so it's assumed that the safety of the wheel is assured.

The final specifications of the wheel are presented in Table 2 and Table 3, enabling an improvement of 9,4 % and 17,7 % respectively, in relation to the market reference value.

Table 2 - Final mass of wheel assembly

Mass (g)			
Wheel	***Hub Assembly***	***Bearing***	***Total***
1537	571,68	78	2264,68

Table 3 - Final rotational inertia of wheel assembly

Rotational inertia (kg.mm²)			
Wheel	***Hub Assembly***	***Bearing***	***Total***
51530	671,118	28,66	52258,438

This shows a considerable reduction of these two important parameters. The final assembly of the wheel with hub is showed in Fig. 20.

Fig. 20 - Final front wheel assembly

IV. CONCLUSION AND FUTURE WORK

In this work, a methodology was developed for optimizing cyclic symmetric geometries. The objective was achieved and the same methodology can be applied on other wheels and similar geometries when using composite materials with fibres. Instead of using big plies covering most of the geometry, this approach enables to apply material where reinforcement is needed for stiffness and later the mass reduction can be optimized for this stiffened geometry.

A methodology to divide the wheel into sections was developed, this eases the consideration of the correct fiber orientation. If this wasn't implemented in design and/or manufacturing, the part would have a non-cyclic symmetric deformation which would induce vibration.

A big reduction was obtained in the reference values of mass and moment of inertia searched, which shows that with optimization techniques there is room for improvement.

As a future work, a rear wheel could be modelled in order to create a set of wheels to be applied in a specific motorcycle. A prototype should be made and tested to validate this methodology and assure safety of the part into the whole assembly. A cost analysis should be done to optimize the manufacturing method.

REFERENCES

1. *ISO 4249-3:2010 – Motorcycle tyres and rims (code-designated series) – Part 3: Rims.*

2. Foale, Tony. *Motorcycle Handling and Chassis Design.* 2002.

3. Altair. Optistruct 12.0 - User guide (2013). *www.altairhyperworks.com.* [Online]

4. *ISO 8644:2006 – Motorcycles - Light-alloy wheels - Test Method.*

5. Brembo finds the answer analysing the F1 and MotoGP braking response on the circuit of Austin. *www.brembo.com.* [Online] 8 4, 2016. [Cited: 12 2, 2016.]

6. Campbell, F.C. *Structural Composite Materials.* s.l. : ASM International, 2010.

7. *Optimization of Blended Composite Wing Panels Using Smeared Stiffness Technique and Lamination Parameters.* Dianzi Liu, Vassili V. Toropov,Ming Zhou,David C. Barton, Osvaldo M. Querin. Orlando, Florida : s.n., 2010, Vols. 51st AIAA/ASME/ASCE/AHS/ASC Structures, Structural Dynamics, and Materials Conference.

8. Reddy, J.N. *Mechanics of Laminated Composite Plates and Shells - Theory and Analysis.* s.l. : CRC Press LLC, 2004.

9. Boyer, Howard E. *Atlas of fatigue curves.* s.l. : ASM International.

10. Jones, Robert M. *Mechanics of Composite Materials, 2nd edition.* s.l. : Taylor & Francis, Inc., 1999.

11. W R Broughton, L E Crocker, M R L Gower. *Design Requirements for Bonded and Bolted Composite Structures.* 2002.